CCCARD2014-XX

MEASUREMENTS IN HORIZONTAL AIR-WATER PIPE FLOWS USING WIRE-MESH SENSORS

É. Lessard, H. Shaban and S. Tavoularis

University of Ottawa, Ontario, Canada

Abstract

The main objective of the present study is the assessment of the measurement uncertainty of void fraction and interfacial velocity in different air-water flow regimes in horizontal pipes, measured by wire-mesh sensors (WMS). New experiments were conducted in a dedicated flow loop and it was found that interfacial velocity measurements by WMS were in good agreement with optical measurements using a high-speed camera. Estimates of the uncertainties of the present void fraction measurements, as well as a review of relevant results from the literature, are also discussed. Drift-flux models were fitted to the present measurements and it was found that the parameters of these models were not only sensitive to the flow regime, but also to the liquid superficial velocity.

Introduction

Multiphase flows, namely, flows of mixtures of two or more distinct phases separated by an interface, are a common occurrence in a variety of industrial and engineering applications. Gas-liquid flows are of particular relevance to the operation and safety analyses of nuclear reactors, including the CANDU (Canada Deuterium Uranium) reactor.

The cores of CANDU reactors are composed of many fuel channels, each containing rod bundles consisting of pellets of nuclear fuel. These fuel channels are housed in a low-pressure vessel, called the calandria. The fuel elements (rods) are cooled by high-pressure heavy water flowing in the fuel channels, which is collected in the outlet header and then directed to the steam generator, where it transfers the absorbed heat to low-pressure light water. The coolant from the steam generator is then fed to the coolant pump, which pressurizes and directs the flow to the inlet headers. The inlet and outlet headers are horizontal tanks connected to the fuel channels by pipes, called feeders. These headers provide steady coolant flow to the fuel channels during normal reactor operation. Throughout this process, the heavy water remains in the liquid phase. In the event of a loss of pressure or a loss of

coolant accident, the reactor is designed to shut down and trigger the Emergency Coolant Injection System (ECIS), which injects high-pressure light water to rapidly enhance the core cooling. In this scenario, however, boiling is expected to occur, resulting in a two-phase gas-liquid flow. The phase distribution in the various feeders under these circumstances is not necessarily uniform, and some fuel channels may receive less liquid to cool the fuel rod bundles than others. To ensure that all the fuel channels are cooled adequately, liquid flow distribution in each of the feeders needs to be measured or predicted accurately.

The velocity distribution of single-phase water flows in pipes can be measured by several well established optical methods, including laser Doppler velocimetry (LDV) and particle image velocimetry (PIV), as well as intrusive methods, such as hot film anemometry [1]. Although a number of techniques have also been developed for the measurement of velocity and phase distributions in gas-liquid flows in pipes, this remains a challenging problem, particularly for systems which do not permit optical access [2,3,4]. The wire-mesh sensor (WMS) method is a promising approach for measuring the quality of gas-liquid flows in pipes, but its application has so far been limited and its measurement uncertainty and extent of its applicability remain under investigation. Although this sensor is an intrusive device, and creates flow disturbance and pressure drop, it has certain advantages compared to alternative approaches. It is not hazardous like radiation methods, it permits multi-sensor measurements at a relatively low cost compared to most optical methods, and does not require flow seeding.

A description of the original wire-mesh sensor and its operation has been provided by the team that developed it [5]. Various modifications and improvements have been made since then, including an increase of its data acquisition rate by an order of magnitude, up to 10 kHz [6], which broadened the range of application the WMS to flows with higher velocities and smaller gas particle sizes. A representative WMS is shown in Figure 1. It consists of two grids of parallel wires (electrodes), perpendicular to each other and to the flow direction. Each grid is positioned on a separate plane and the two planes are separated stream-wise by a short distance of roughly 2 mm. This device measures the local instantaneous conductivity of the flowing mixture at the nodes of the mesh formed by the two grids. An electronic control system sends electric current pulses sequentially through each of the electrodes of the upstream grid and a multi-plexed data acquisition system records the electric potential differences between each pair of perpendicular wires in the two grids. At nodes at which air occupies some or all of the space between the two wires, the conductivity of the material between the two wires would be lower than that of water and so the gas phase would be detected at that node. The phase detection at all nodes is completed simultaneously at a rate that is sufficiently fast for the system to measure essentially instantaneous phase maps in a cross section of the flow. The addition of a second WMS downstream of the first one makes it possible to measure the convection speed of the interface between the two phases.

The work presented in this paper is in support of the AECL header/feeder research, specifically in the study of horizontal air-water pipe flow. It is part of a research program at the University of Ottawa, which includes both experimental and numerical studies of air-water flows in horizontal and vertical pipes and in simplified header/feeder models.

Niagara Falls Marriott Fallsview Hotel & Spa, Niagara Falls, Ontario Canada, April 27-30, 2014.

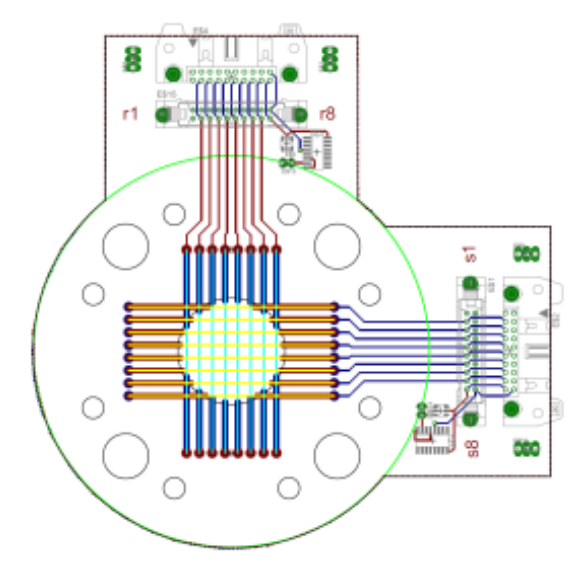


Figure 1 An 8×8 wire-mesh sensor.

1. Uncertainty of void fraction measurements by WMS

Several published studies have compared the uncertainty of void fraction measurements made using WMS with those made using other methods, especially in vertical upward air-water flows. In the introductory paper about the WMS [5], the authors compared the centre-line averaged void fraction measured by the WMS to that measured using a single-beam gamma ray densitometer and an electrode mesh sensor. This work identified a systematic positive bias of 8% in the absolute void fraction measured by WMS by comparison to measurements by the two other methods (Figure 2). In another study using a gamma ray densitometer [7] the investigators traversed the gamma ray device along the pipe diameter, such that the gamma ray beam was always located just below one of the WMS wires. This allowed a comparison of the chordal void fraction in the entire pipe cross-section and the authors found that the WMS void fraction measurements exceeded significantly those of the gamma ray densitometer near the pipe wall.

Comparisons of the void fraction distributions measured by a WMS and an X-ray Computerized Tomography (CT) system were performed by Prasser *et al.* [8] and Zhang *et al.* [9]. Although the X-ray CT is a relatively new measurement method compared to the gamma ray densitometer, which has been used in gas-liquid flow measurements for more than 50 years, it has a superior temporal resolution and a spatial resolution that is higher than that of the WMS. In general, the two methods produced very similar phase distributions (Figure 3), except for the tendency for the WMS to overestimate the void fraction near the wall. Additionally, Prasser *et al.* [8] showed that the WMS slightly underestimated the void fraction inside Taylor bubbles during slug flow conditions and caused a deformation of the Taylor bubbles at low liquid superficial velocities. Both studies showed that the cross-section averaged void fractions measured by the two methods were within 5% of the absolute void fraction.

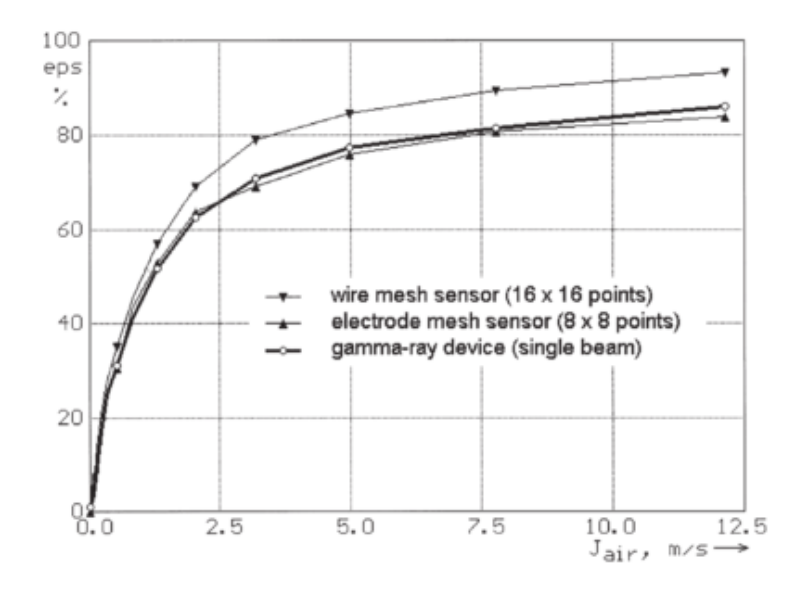


Figure 2 Centre-line averaged void fractions measured at different air superficial velocities by wiremesh sensor, electrode mesh sensor and gamma ray densitometer [5].

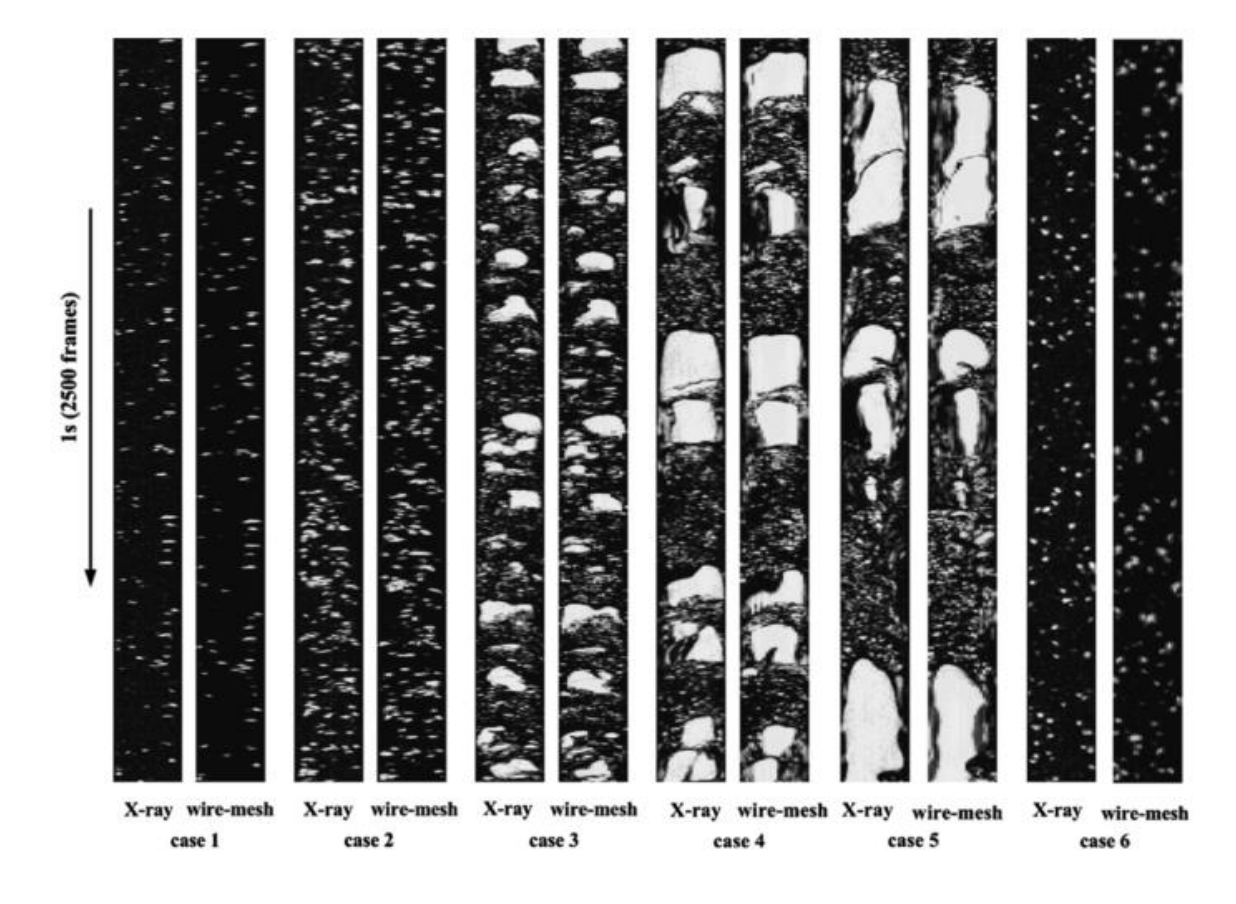


Figure 3 Comparison of axial void fraction distributions measured by X-ray CT and WMS [9].

Other methods have also been used for more detailed uncertainty analyses of void fraction measurements by WMS. Manera *et al.* [10] compared WMS void fraction measurements to those measured using conductive needle probes, which give highly accurate point measurements of void fraction. Comparisons of void fraction measurements with those of recently developed tomographic techniques, including electrical capacitance tomography (ECT) [11] and electrical resistance tomography (ERT) [12], can also be found in the literature. In all these studies, good agreement was generally found in the absolute cross-section averaged void fraction measured by the WMS and the other methods, however, relative differences were high in some cases. Also, some discrepancies were found in the measured local void fractions, especially near the pipe walls, which were attributed to the limited spatial resolution of the WMS and the sharp changes in void fraction that occur near pipe walls.

2. Experimental facility and instrumentation

The WMS was tested in an air-water flow loop in the Fluid Mechanics Laboratory, at University of Ottawa (Figure 4). Water from a containment tank was pumped to the head tank, 4.5 m above the test section. The head tank was partitioned by a vertical dividing wall, which acted as an overflow and maintained a constant head to the test section, whereas excess water was redirected to the containment tank. The water flow rate was measured by an ultrasonic water flowmeter and the air volumetric flow rate was measured by a rotameter. Air from the University's compressed air system was injected into the water flow through a nozzle just downstream of the pipe inlet. The water and air flow rates were adjusted to generate flows in different two-phase flow regimes, including bubbly, slug and annular flows, as well as transitional regimes. Some of the main specifications of the loop are listed in Table 1.

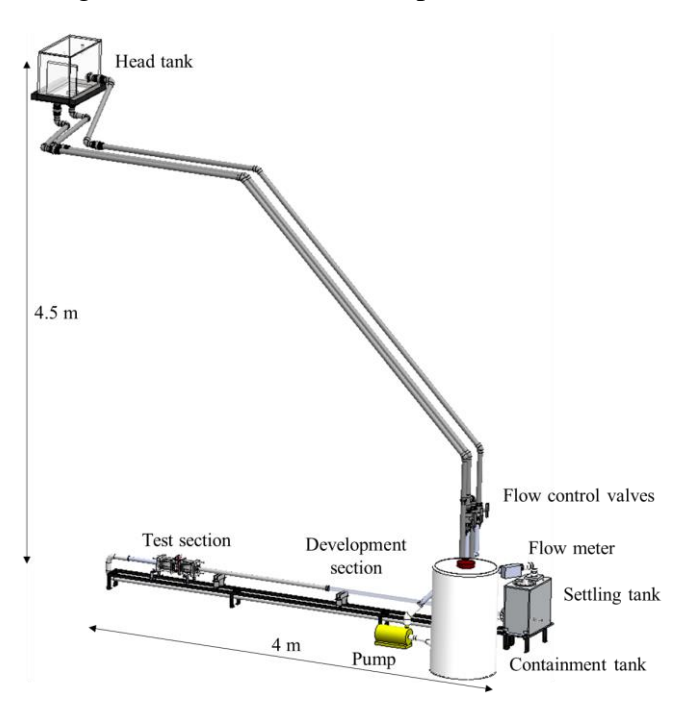


Figure 4 Air-water flow loop.

Head tank height above test section	4.5 m
Test section I.D.	D = 31.75 mm (1.25 in)
Development section length	3.15 m (97 <i>D</i>)
Test section length	0.38 m (12 <i>D</i>)
Containment tank volume	225 liters
Water operating temperature	$T = 22 \pm 2$ °C
Maximum water superficial velocity	$j_l \approx 3 \text{ m/s}$
Maximum air superficial velocity	$j_g \approx 15 \text{ m/s}$

Table 1 Air-water flow loop main specifications.

Figure 5 illustrates the test section, which was positioned downstream of a long pipe (1), which allowed full development of the air-water flow. The test section contained a pair of WMS (2) mounted on a special flange (3). The WMS used in this project had an inner diameter of 31.9 ± 0.2 mm, and consisted of an 8×8 array of wires with a diameter of 0.24 ± 0.02 mm and spaced centre-to-centre by 3.8 ± 0.4 mm. The sensor operated at a measurement frequency of 10 kHz. The upstream and downstream sensors were separated by an axial distance of 22.7 ± 0.3 mm. On either side of the WMS assembly, there were two short pipe sections (4) with 0.7 mm thick walls made of fluorinated ethylene propylene (FEP, also known by the trade name Teflon), having a refractive index that matches that of water, thus allowing undistorted optical access. The FEP pipe sections were immersed in square viewing tanks with glass walls (5) and containing still water (6). Additional details for the facility, instrumentation and experimental procedures have been reported elsewhere [13].

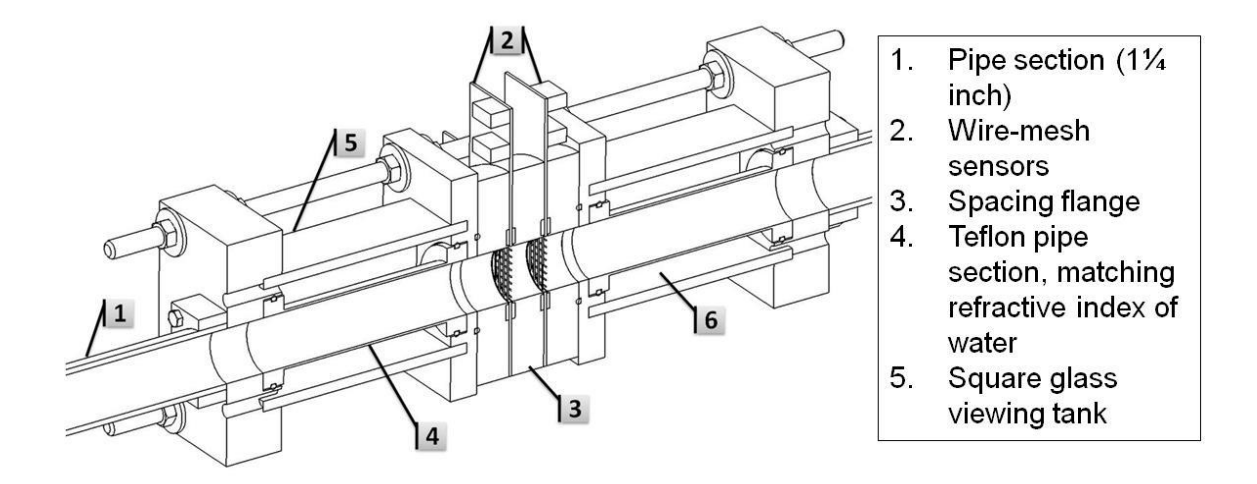


Figure 5 The test section and its main components.

3. Results

A total of 300 measurements were made for different combinations of liquid superficial velocity in the range from 0.2 m/s to 3 m/s and gas superficial velocity in the range from 0.1 m/s to 15 m/s. The flow regime for each measurement, identified by visual inspection, was noted and the flow regime map shown in Figure 6 against axes of liquid and gas superficial velocities was constructed. Contours enclosing measurements in each flow regime were drawn and the areas enclosed by each contour have been marked by different colours. The shapes of these contours are approximate, as there was overlap between neighbouring regimes, possibly corresponding to transitional states. At a constant liquid superficial velocity, transitions from one regime to the next were fairly consistent, except at the higher liquid superficial velocities where the flow transitioned directly from slug flow to misty annular flow rather than to stratified wavy flow. The average void fraction $\bar{\epsilon}$, measured by the upstream WMS, has been plotted vs. the liquid superficial velocity j_l in Figure 7, which also shows lines of constant gas superficial velocity j_g . It is noted that the majority of the measurements were taken at relatively high void fractions.

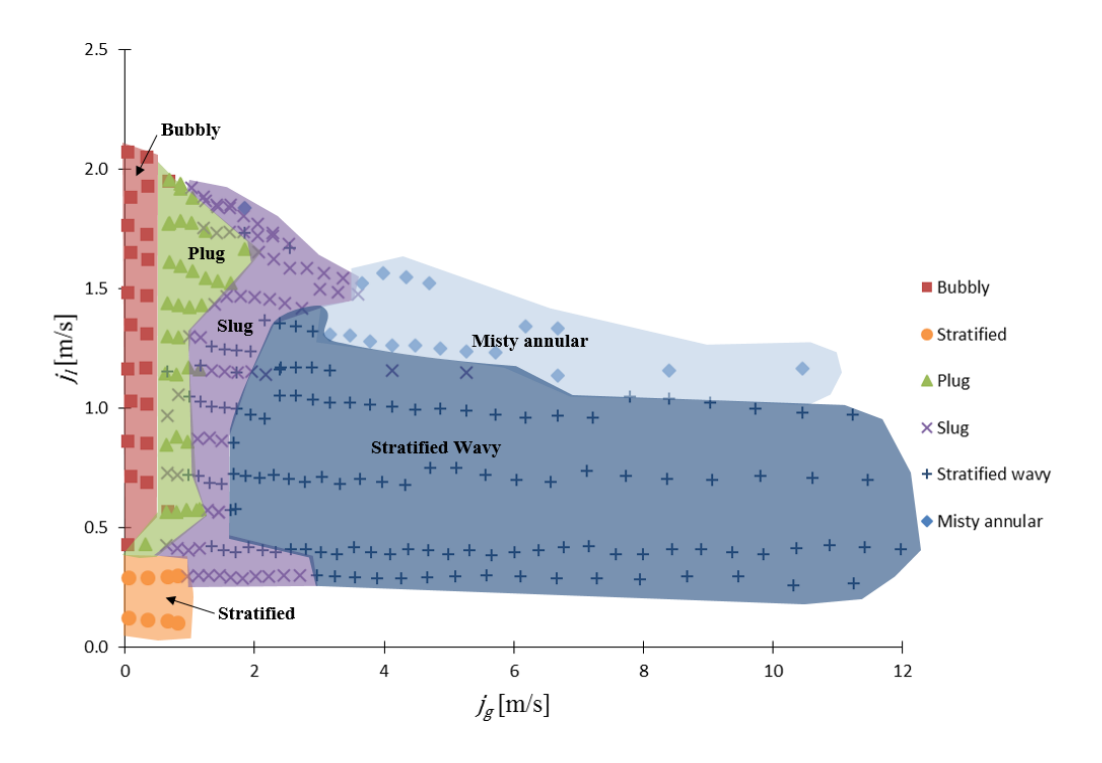


Figure 6 Air-water flow regime map for the present study.

Niagara Falls Marriott Fallsview Hotel & Spa, Niagara Falls, Ontario Canada, April 27-30, 2014.

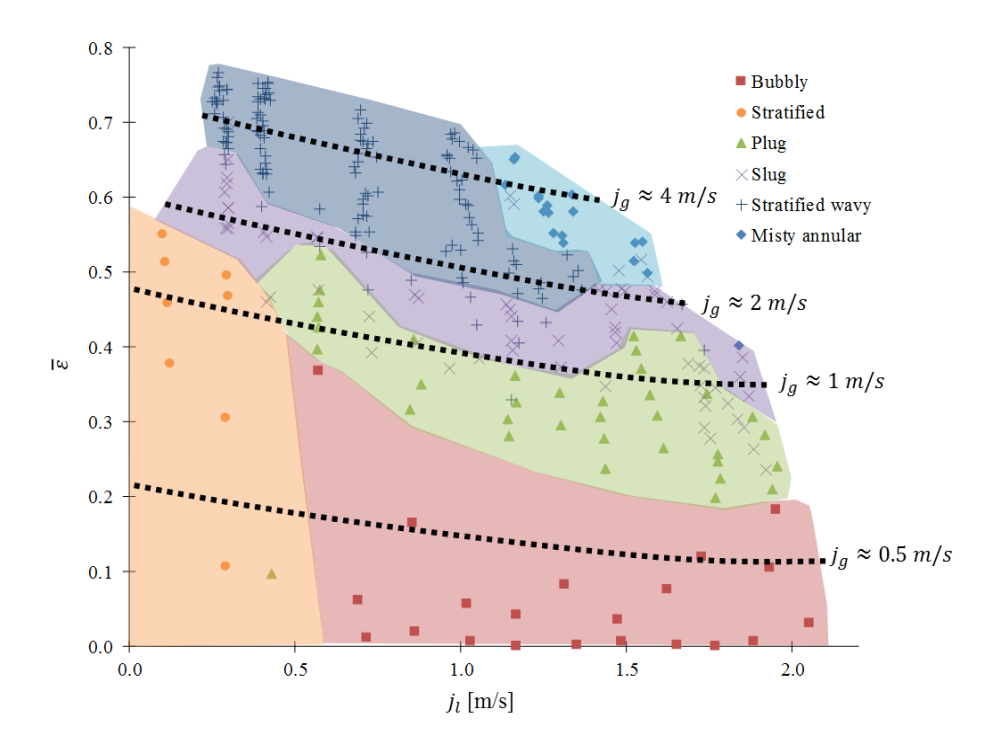


Figure 7 Average void fraction vs. water superficial velocity for different flow regimes.

Measurements of the interfacial velocity were made by correlating the outputs of the two WMS in the test section. Independent measurements of the interfacial velocity were also made by tracking the air-water interface on successive images recorded with a high-speed camera. The later method was only used for sparse bubbly flows, for which it was possible to track photographically individual bubbles and determine their average velocity between an upstream and downstream location of the test section. A comparison of selected WMS measurements of the average liquid-gas interfacial velocity and corresponding photographic results in bubbly flows is shown in Figure 8. The straight black dotted line represents the limiting condition for which the liquid superficial velocity and the interfacial velocity would be equal. The results for both measurement techniques are shown together with the corresponding uncertainty bars at 95% confidence level, i.e., equal to twice the corresponding standard deviation. A fairly good agreement between the two measurement techniques is observed over the entire range of liquid superficial velocity. The uncertainty of the WMS measurements was higher than the one from high speed camera. This is attributed to three sources: first, the number of distinct interfaces measured by the WMS was at least ten times higher, thus introducing a larger statistical scatter; second, the WMS measurement took into consideration all bubbles detected, including the very small ones, which were difficult to track by high-speed photography; and, third, that the WMS measured the average interfacial velocity over the relatively short distance between the two sensors (roughly 20 mm), whereas the high speed camera measured it over the longer distance from the upstream and downstream end of the test section (roughly 180 mm).

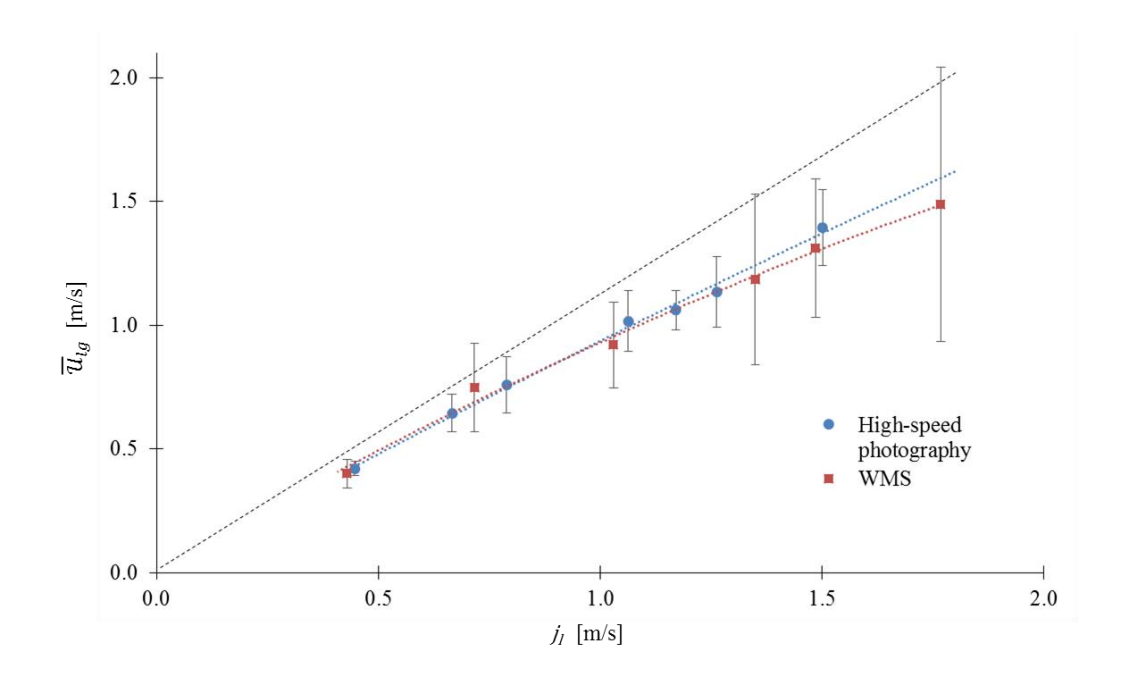


Figure 8 Interfacial velocities measured by high-speed photography *vs.* WMS measurements in bubbly flow; bars indicate estimated uncertainties.

A concern when using WMS is that their physical presence introduces flow distortion. In particular, air bubbles passing through the wires of the sensor get deformed and may possibly break up. Some insight into the flow disturbance by the WMS may be gained by comparison of measurements by the upstream and downstream sensors. Figure 9 shows the difference between the average void fraction measured by the upstream and downstream sensors plotted *vs.* the water superficial velocity. In most cases, the upstream sensor measured a larger void fraction than the downstream one. Larger deviations occurred at superficial water velocities lower than 1 m/s and the measurement difference tended to decrease with increasing liquid superficial velocity. Because the upstream sensor encounters a flow which is less affected by the intrusiveness of the device than the downstream sensor is, its void fraction measurements are expected to be more representative of the flow upstream of the test section. For this reason void fraction measurements presented in this paper were taken with the upstream sensor only.

As an additional illustration of the flow distortion introduced by WMS, Figure 10 shows measurements of interfacial velocity by the high-speed camera upstream of, across, and downstream of the WMS pair for the range of liquid superficial velocities between 0.5 m/s and 1.5 m/s. The downstream velocities were consistently and significantly (typically by about 40%) higher than those upstream of the WMS. Across the sensors (near-WMS), the velocity increased, suggesting acceleration of the interface during crossing of the sensor arrays. At lower j_l , the downstream velocities nearly coincided with the near-WMS velocities, but at higher j_l the downstream velocities exceed measurably the near-WMS velocities.

Niagara Falls Marriott Fallsview Hotel & Spa, Niagara Falls, Ontario Canada, April 27-30, 2014.

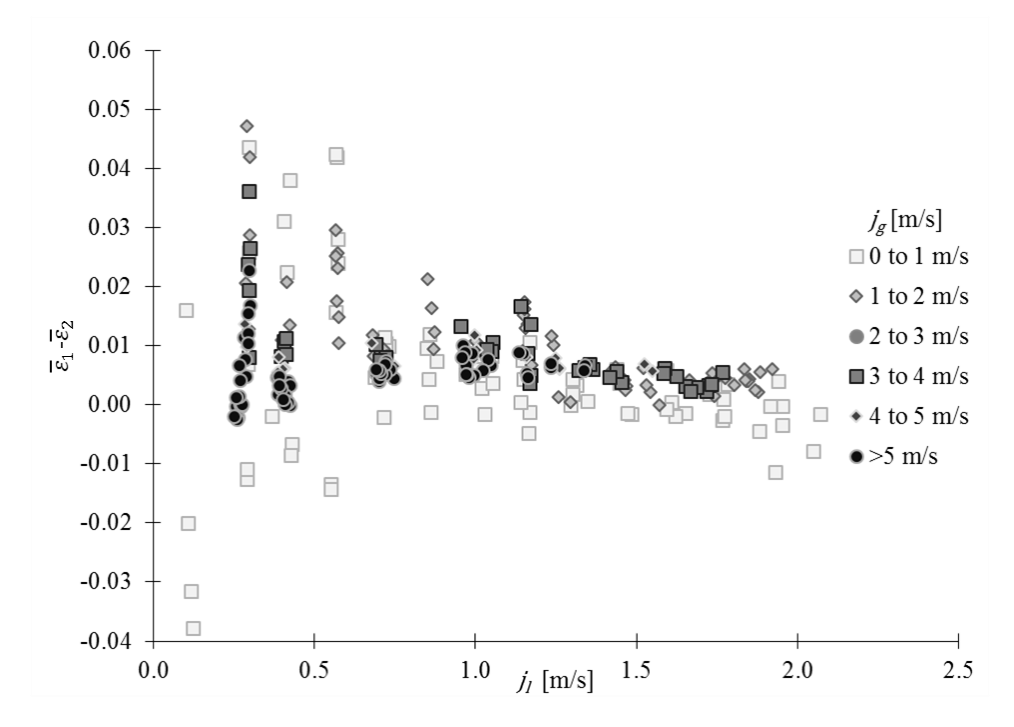


Figure 9 Difference between average void fractions measured by the upstream and downstream sensors.

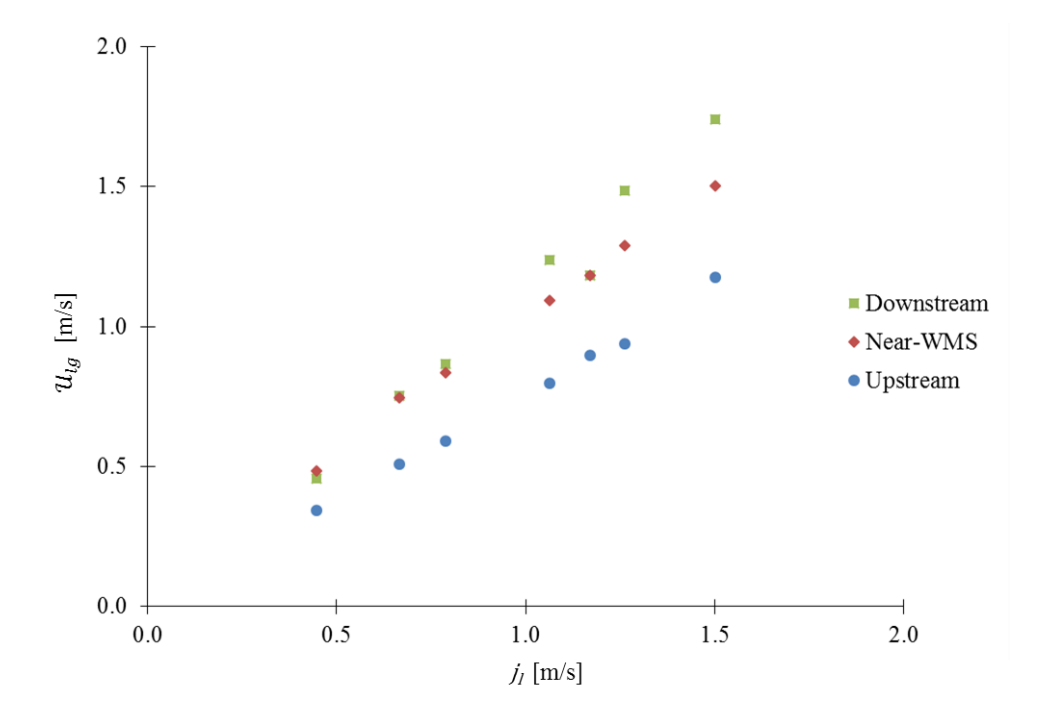


Figure 10 Interfacial velocities measured by the high-speed camera upstream, downstream and near the WMS.

4. Development of drift-flux models

The drift flux model is a simple and widely used empirical method of correlating the void fraction ε and the gas j_g and total j superficial velocities [14]. A convenient form of drift flux models is

$$j_g/\varepsilon = c_0 j + v_{gj} \tag{1}$$

where c_0 is a correction factor that accounts for velocity and void fraction non-uniformities across the channel and v_{gj} represents the difference between the gas velocity and the total superficial velocity. The values that fitted best to the full set of present measurements were $c_0 = 1.4$ and $v_{gj} = 0.13$ m/s, while those fitted to each flow regime are listed in Table 2. The drift-flux parameters for each group of measurements taken at a roughly constant liquid superficial velocity j_l are listed in Table 3 in ascending order and with the flow regimes indicated. The average percent and RMS differences between predictions of these models were significantly lower than those of models based on flow regime grouping. This indicates that the drift flux parameters are not only specific to flow regime, but they are also sensitive to the liquid superficial velocity.

Regime	c_0	v_{gj} [m/s]	Average percent difference	RMS difference	# of data points
Stratified	1.7	-0.07	-1.0 %	9.7 %	7
Plug	1.3	0.01	-4.9 %	9.6 %	35
Slug	1.5	-0.25	-5.0 %	9.1 %	66
Stratified wavy	1.4	0.02	-3.1 %	5.8 %	135
Misty annular	1.5	-0.50	-6.7 %	7.1 %	18

Table 2 Drift-flux model parameters estimated from measurements in each flow regime and average percent and RMS differences between measured values and model predictions.

Dominant flow regime(s)	j_l [m/s]	c_{θ}	<i>v_{gj}</i> [m/s]	Average percent difference	RMS difference	# of data points
Slug, Stratified Wavy	0.28	1.3	0.24	-1.2 %	1.7 %	37
Stratified Wavy	0.40	1.3	0.13	-0.7 %	1.1 %	37
Stratified Wavy	0.71	1.4	-0.15	-0.7 %	0.7 %	30
Stratified Wavy	1.00	1.4	-0.36	-0.8 %	0.8 %	30
Stratified Wavy, Annular Misty	1.29	1.5	-0.74	-0.6 %	0.6 %	22
Plug	1.57	1.6	-1.05	-0.4 %	0.5 %	17
Plug, Slug	1.88	1.7	-1.6	-0.2 %	0.5 %	7

Table 3 Drift-flux model parameters estimated from measurements at constant j_l and average percent and RMS differences between measured values and model predictions.

5. Summary and conclusions

This research has been motivated by the current need in the industry for reliable prediction and measurement methods for two-phase flows in header/feeder systems. As a contribution to address this issue, an air-water flow loop was designed to allow void fraction and interfacial velocity measurements in horizontal flows using wire-mesh sensors and high-speed photography. In order to obtain fully-developed flow in the test section in a consistent and repeatable fashion, a long development section and a head tank to maintain constant head pressure were used. The flow loop was able to successfully reproduce a wide range of horizontal flow regimes of interest, except for annular flow due to the water flow rate limitations.

Void fraction measurements by two wire-mesh sensors, one positioned downstream of the other, were found to be in good agreement at high gas and liquid superficial velocities, but differed significantly at low superficial velocities. For this reason, all reported void fraction measurements were taken with the upstream sensor, which is exposed to a flow that is less disturbed by the intrusion of the device than its downstream counterpart.

Interfacial velocity measurements were performed using a pair of wire-mesh sensors in bubbly, slug and plug flows, but not in stratified, wavy and annular flows, in which many nodes of the sensor were never or seldom crossed by the air-water interface. Average interfacial velocity measurements obtained by photography at low void fractions were in good agreement with those from the WMS. The uncertainties of both methods increased with increasing liquid velocity.

Drift flux model parameters were proposed based on the overall population of measurements, by flow regime grouping as well as by liquid superficial velocity grouping, and the average percent and RMS differences were determined. The distribution parameter c_0 generally increased as the liquid superficial velocity j_l increased. On the other hand, the drift velocity parameter v_{gj} generally decreased as j_l increased. As a result, when combining measurements sorted by flow regime, a fairly large RMS difference was observed. Alternatively, much smaller errors were observed when the drift flux parameters were derived for groups of measurements taken at a constant liquid superficial velocity j_l . These observations suggest that the drift-flux parameters c_0 and v_{gj} would be sensitive to the liquid superficial velocity, and that drift-flux models based solely on flow regime would not be sufficient to accurately predict the void fraction over all ranges of flow rate.

Acknowledgement

This work has been supported by Atomic Energy of Canada Ltd. (AECL), the University Network of Excellence in Nuclear Engineering (UNENE) and the Natural Sciences and Engineering Research Council of Canada (NSERC).

6. References

[1] Tavoularis. S. (2005). *Measurement in Fluid Mechanics*. Cambridge University Press, Cambridge, UK.

- [2] Balachandar, S. and Eaton, J. K. (2010). "Turbulent Dispersed Multiphase Flow," *Ann. Rev. Fluid Mech.* **42**, 111–133.
- [3] Collier, J. G. and Thome, J. R. (1994). *Convective Boiling and Condensation*. Oxford University Press, New York, USA.
- [4] Crowe, C. T. (2006). *Multi-phase Flow Handbook*. CRC Press, Taylor & Francis, Boca Raton, Florida, USA.
- [5] Prasser, H.-M., Böttger, A., and Zschau, J. (1998). "A New Electrode-Mesh Tomograph for Gas-Liquid Flows," *Flow Meas. Instrum.* **9**, 111-119.
- [6] Prasser, H.-M., Zschau, J., Peters, D., Pietzsch, G., Taubert, W., Trepte, M. (2000). "Wiremesh sensor now 10,000 frames per second," *Annual Report 1999*, Institute of Safety Research, FZR-284, Feb. 2000, ISSN 1437-322X, 15-18.
- [7] Sharaf, S., Da Silva, M., Hampel, U., Zippe, C., Beyer, M. and Azzopardi, B. (2011), "Comparison between wire mesh sensor and gamma densitometry void measurements in two-phase flows," *Meas. Sci. Technol.*, **22**, doi:10.1088/0957-0233/22/10/104019.
- [8] Prasser, H.-M., Misawa, M. and Tiseanu, I., (2005). "Comparison between wire-mesh sensor and ultra-fast X-ray tomograph for an air-water flow in a vertical pipe," *Flow Meas. Instrum.*, **16**, 73–83.
- [9] Zhang, Z., Bieberle, M., Barthel, F., Szalinski, L. and Hampel, U., (2013). "Investigation of upward cocurrent gas—liquid pipe flow using ultrafast X-ray tomography and wire-mesh sensor," *Flow Meas. Instrum.*, **32**, 111–118.
- [10] Manera, A., Ozar, B., Paranjape, S., Ishii, M. and Prasser, H.-M., (2009). "Comparison between wire-mesh sensors and conductive needle-probes for measurements of two-phase flow parameters," *Nucl. Eng. Des.*, **239**, 1718–1724.
- [11] Azzopardi, B. and Abdulkareem, L., (2010). "Comparison between electrical capacitance tomography and wire mesh sensor output for air/silicone oil flow in a vertical pipe," *Ind. Eng. Chem. Res.*, **49**, 8805–8811.
- [12] Olerni, C., Jia, J. and Wang, M., (2013). "Measurement of air distribution and void fraction of an upwards air—water flow using electrical resistance tomography and a wire-mesh sensor," *Meas. Sci. Technol.*, **24**, doi:10.1088/0957-0233/24/3/035403.
- [13] Lessard, É., (2014). "Measurements in horizontal air-water pipe flows using wire-mesh sensors," M.A.Sc. Thesis, Department of Mechanical Engineering, University of Ottawa, Ottawa, Ontario, Canada.
- [14] França, F. and Lahey Jr., R. T. (1992). "The use of drift-flux techniques for the analysis of horizontal two-phase flows," *Int. J. Multiphase Flow* **18** (6), 787-801.